Ergodicity Test of the Eddy Correlation Method

Jinbei CHEN[1] Yinqiao HU[1] Ye YU[1] Shihua LÜ[1]

[1] *Key Laboratory of Land Surface Process and Climate Change in Cold and Arid Regions; Cold and Arid Regions Environment and Engineering Institute, Chinese Academy of Sciences, Lanzhou 730000,P R China.*

E-mail: chenjinbei@lzb.ac.cn

Abstract

In this paper, two sets of data from the Nagqu Station of Plateau Climate and Environment (NaPlaCE) and the cooperative atmosphere-surface exchange study 1999 (CASES-99) were used to analyze and verify the ergodicity of turbulence measured by the eddy covariance system. The results show that the eddies of atmospheric turbulence that are smaller than the scale of the atmospheric boundary layer (i.e. the spatial scale is less than 1,000 m and temporal scale is shorter than 10 min) can effectively satisfy the conditions of the average ergodic theorem, and belong to a wide ergodic stationary random processes. Meanwhile, the eddies, of which the spatial scale are larger than the scale of boundary layer, cannot satisfy the conditions of the average ergodic theorem, and thus it involves non-ergodic stationary random processes. Consequently, when the finite time average was used to substitute for the ensemble average, a large rate of error would occur with use of the eddy correction method due to the losing the low frequency component information of the larger eddies. When the multi-station observation was compared with the single-station observation, then the wide ergodic stationary random process originating from the multi-station observation expanded from the eddies which were 1000 m smaller than a boundary layer scale to the eddies, which were larger than the boundary layer scale of 2000 m. Therefore, the calculation of the turbulence average or variance and turbulent flux could effectively satisfy the ergodic assumption, and the results would be approximate to the actual values. Regardless of vertical velocity and temperature, if the ergodic stationary random processes could be satisfied, then the variance of the eddies in the different temporal scales could follow M-O similarity relations; in the case of the non-ergodic random process, the eddies variance deviated from the M-O similarity relations.

Keywords: Ergodic assumption; eddy correlation method; M-O similarity relations;

atmospheric surface layer (ASL); high-pass filtering

1 Introduction

The basic principle of the turbulence measurement average is the ensemble average of space, time and state. However, it is impossible to set numerous observational instruments in space and have enough time to obtain all states of the turbulent eddy to realize the ensemble average in actual turbulence measurement experiments. Therefore, based on the ergodic assumption that it is temporally steady and spatially homogeneous, the time average of one spatial point, which is long enough for observation, was used to substitute for the ensemble average (Stull 1988; Wyngaard 2010; Aubinet 2012). The ergodic assumption was first raised by Boltzmann (Boltzmann 1871; Uffink 2004) in his study of ensemble theory of statistical dynamics. He argued that an isolated system began from any initial state would undergo all possible microstates after a certain amount of time. At the beginning of the 20th century, the P. Ehrenfest duo proposed the quasi-ergodic hypothesis and changed the term “experience” in the aforesaid ergodic hypothesis to “infinitely approximate”. The basic point of the ergodic hypothesis or quasi-ergodic hypothesis was recognizing that the macroscopic property of the system in the equilibrium state was the average of the microcosmic quantity in a certain amount of time. Nevertheless, the ergodic hypothesis or quasi-ergodic hypothesis was never proven theoretically. The proof of the ergodic hypothesis in physics aroused the interest of mathematicians, and Neumann et al. (1932) first theoretically proved the ergodic theorem (Birkhoff 1931) in topological space. Krengel (1985) then systematically summarized related achievements. However, the ergodic theorem expressed in the time series by the theory of stationary random process is further intuitionistic in physics. The stationary random process is a random process in which the statistical properties do not vary with time. When the limit of the autocorrelation function of the stationary random process converges to its average square, this random process is ergodic, this is namely the ergodic theorem of the stationary random process. The ergodic theorem also provides the necessary and sufficient conditions for the ergodicity of the stationary random process. Mattingly (2003) reviewed the research progress of ergodicity of random Navier-Stokes equations which had been made in recent years, and Galanti (2004) solved the random Navier-Stokes equation by numerical value simulation to

prove that the turbulence which was temporally steady and spatially homogeneous was ergodic (Lennaert et al. 2006). However, he also indicated that such partially turbulent flows acting as mixed layer, wake flow, jet flow, flow around and boundary layer flow may be non-ergodic turbulence.

The ergodic hypothesis is a basic hypothesis in atmospheric turbulent experiment. Stationarity, homogeneity, and ergodicity are routinely used to link the ensemble statistics (mean and higher-order moments) of turbulence field measurements collected in the ASL and CSL to land surface processes. Many literatures habitually referred to the ergodic assumption, as some descriptions such as “when satisfying ergodicity hypothesis, ……” or “something indicates that ergodicity hypothesis is satisfied”. Though the evidence of the validity of the ergodic hypothesis in the ASL is just the success of Monin-Obukhov (M-O) similarity theory for unstable and near-neutral conditions, the success of similarity theory, as only a necessary condition for ergodicity in the ASL, does not prove ergodicity (Katul et al., 2004). Katul et al. (2004) qualitatively analyzed the problems in ergodicity regarding atmospheric turbulence, and believed that it was common for neutral and unstable stratified atmosphere in the surface layer to reach ergodicity, while it was difficult for the stable layer to reach ergodicity. The lidar technique opens up new possibilities for atmospheric measurements and analysis by providing simultaneous high-resolution spatial and temporal atmospheric information (Eichinger et al., 2001). The stationarity and ergodicity can be tested for such ensembles of experiments. Recent advances in LIDAR (Light Detection and Ranging) measurements offer a promising first step for direct evaluation of such hypotheses for ASL flows (Light Detection and Ranging) measurements offer a promising first step for direct evaluation of such hypotheses for ASL flows (Higgins et al., 2013). Higgins et al. (2013) apply a water vapor concentration lidar to investigate the ergodic hypothesis of atmospheric turbulence for the first time. But no author did perform quantitative testing or theoretical demonstration of the eddy covariance system related to the ergodicity of the atmospheric turbulence. Therefore, it is clear that there is a need to reevaluate turbulence measurement technology, to test the ergodicity of atmospheric turbulence quantitatively by means of observation experiments. Obviously, the advances of research on the ergodicity in the mathematics and physics are far more quickly than the atmospheric science. We try firstly to introduce the ergodic theorem of the

stationary random processes to atmospheric turbulence in surface layer in this paper to analyze and verify the ergodicity of turbulence measured by the eddy covariance system.

The land surface process, of which the core is mass-energy exchange, between ecosystem and atmosphere under complicated conditions, has been a scientific issue which urgently requires study in the fields of atmospheric science, ecology, geography science, etc. (Running et al. 1999; Geider et al. 2001). A core goal of FLUXNET and relevant scientific research is to determine the turbulent flux of mass (moisture and CO_2) and energy (sensible heat and latent heat) between ecosystem and atmosphere, and thus the eddy correlation method, which is used to measure atmospheric turbulent flux, is widely applied (Baldocchi et al. 2001). Being generally based on the assumed constant flux layer, and Monin–Obukhov (M–O) similarity theory, the whole layer atmospheric turbulent flux is determined by eddy correlation in the atmospheric surface layer. According to the spectral gap (around 60 min) between the turbulence scale and synoptic scale of the wind velocity spectrum in the atmospheric surface layer, so firstly the trend correction of observational data (McMillen 1988; Moore 1986) is done to eliminate the interference of synoptic scale motion during the turbulence observation. After the observation errors of the instruments had been eliminated, the average, $\bar{u}$, was determined within 15-60 min, the turbulence component, $u' = u - \bar{u}$, was obtained, and finally the turbulent flux of the mass and energy between ecosystem and atmosphere was calculated and determined by means of variance and covariance. With respect to the M-O similarity theory, the constant flux layer requires that the flow field is steady and homogeneous, i.e. the average vertical velocity does not exist. Therefore, many experiments of atmospheric boundary layer focus on seeking ideal homogeneous surface as much as possible. When the vertical velocity occurs in experiment, the coordinate rotation is highlighted in the error correction of the eddy correlation method (Finnigan 1983; Wilczak et al. 2001) to eliminate it. The original motive of the coordinate rotation is to eliminate the vertical velocity caused by the tilt of instrument installation. However, the turbulent flux is often measured under complex terrain conditions in FLUXNET, and even the large eddy can cause the vertical velocity over homogeneous surface. The coordination rotation in the error correction will eliminates the effects of the average vertical velocity caused by the terrain and large eddy in the turbulent flux. After

analysis, Finnigan (2004) found that the rotation of coordination eliminated the low frequency effect caused by natural terrain. Evenly, the large eddy can cause the vertical velocity over homogeneous surface. The rotation of the coordination in the error correction will eliminates the effects of the average vertical velocity of terrain and large eddy on the turbulent flux. When surface energy imbalance, NEE (Net Ecosystem Exchange) estimation error, and other problems occurred, and it was necessary to consider the low frequency effect (Foken et al. 2006; Segal et al. 1988; Mahrt et al. 1993; Sun et al. 1997; Finnigan et al. 1995; Sakai et al. 2001; Malhi et al. 2004; Chen et al. 2006), and many methods were proposed to estimate the low frequency effect of the transport flux eddy (Lee 1998; Zhang et al. 2010; Baldocchi 2000; Aubinet et al. 2003; Staebler et al. 2004; Hu 2003; Chen et al. 2007; Chen et al. 2013). In the rotation of coordinates for correction in the eddy correction method, eliminating the average vertical velocity and estimating the low frequency effect of the eddy of the transport flux were essentially contradictory. According to Kaimal and Wyngaard (1990), the atmospheric turbulence theory and observation method were feasible and led to success under ideal conditions (including a short period, steady state and homogeneous underlying surface, and through observation in the 1950s-1970s) but these conditions are rare in reality. In the land surface process and ecosystem, the observations must be implemented under conditions such as with complex terrain, heterogeneous surface, long period and unsteady state. The above experimental studies imply that the turbulence should be divided into some eddies with different scales in the meticulous study. It is necessary that more modern observational tools and theories will be applied with new perspectives in future research.

In the spatial scale, the atmospheric turbulence from the dissipation range, inertial sub-range to energy range, and further large eddy of turbulent flow is extremely broad (Stull 1988). Such spatial and temporal size of eddies include the isotropous 3-D eddy structure of high frequency turbulence and orderly coherent structure of low frequency turbulence (Li et al. 2002). The eddies in different scales are also different in terms of their spatial structure and physical properties, and even their transport characteristics are not all the same. It is thus reasonable that the eddies with different transport characteristics are separated, processed and studied by using different methods (Zuo et al. 2012).

Based on the aforesaid analysis, in this study the data from the Nagqu Station of Plateau Climate and Environment were used to measure turbulence by the eddy correlation method under the homogeneous surface and the Fourier transform band-pass filtering method was used to make filtering of different scales. Then the ergodicity of different scale eddies of atmospheric turbulence were directly tested quantitatively on the basis of the observational data. In addition, the cooperative surface layer turbulence data of the Kansas, US prairie (CASES-99) were used to verify the ergodicity of the turbulence measured by multi-station observations. The characteristics of the M-O variance similarity relations of the eddies in different scales were compared and analyzed to test the feasibility of the M-O similarity of the ergodic and non-ergodic turbulence. The problems of the eddy correlation method in the atmospheric turbulence observation in the surface layer were further explored on the basis of the study on the ergodicity and M-O variance similarity relations of the eddies in different scales in this paragraph in order to provide an experimental basis for utilizing the M-O similarity theory and developing the transport theory of turbulence in atmospheric boundary layers with complex underlying surfaces.

2 Theories and methods

2.1 Ergodic theorem of stationary random process

The stationary random process is a random process which will not vary with time, i.e., for observed quantity A, its spatial x_i and temporal t_i functions satisfy the following conditions:

$$A(x_1, x_2, \ldots, x_n; t_1, t_2, \ldots, t_n) = A(x_1, x_2, \ldots, x_n; t_1+\tau, t_2+\tau, \ldots, t_n+\tau), \quad (1)$$

where τ is a time period, defined as the relaxation time.

The average μ_A of random variable A and autocorrelation function $R_A(\tau)$ are respectively defined as follows:

$$\mu_A = \lim_{T\to+\infty} \frac{1}{T}\int_0^T A(t)dt\,, \quad (2)$$

$$R_A(\tau) = \lim_{T\to+\infty} \frac{1}{T}\int_0^T A(t)A(t+\tau)dt\,. \quad (3)$$

Autocorrelation function $R_A(\tau)$ is a temporal second-order moment. In the case of τ=0, the autocorrelation function $R_A(\tau)$ is the variance of a random variable. The necessary and sufficient condition of the stationary random process average to have ergodicity is the average ergodic function Ero(A) (Papoulis et al. 1991), as shown below:

$$\mathrm{Ero}(A)=\lim_{T\to\infty}\frac{1}{T}\int_0^{2T}\left(1-\frac{\tau}{2T}\right)\left[R_A(\tau)-\mu_A^2\right]d\tau=0. \tag{4}$$

The average ergodic function Ero(A) is the time integral of variance between autocorrelation function $R_A(\tau)$ of variable A and its average, μ_A. If the average ergodic function Ero(A) converges to zero, then the stationary random process will be ergodic. In other words, if the autocorrelation function $R_A(\tau)$ of variable A converges to the square of its average μ_A, this stationary random process is average ergodic. Equation (4) is the average ergodic theorem. For discrete variables, Eq. (4) can be rewritten as the following:

$$\mathrm{Ero}(A)=\lim_{n\to\infty}\sum_{i=0}^{n}\left(1-\frac{\tau_i}{n}\right)\left[R_A(\tau_i)-\mu_A^2\right]=0. \tag{5}$$

Equation (5) is the average ergodic theorem of the discrete variable. Hence, Eqs. (4) and (5) can be used as the basis to determine the average ergodicity.

The necessary and sufficient condition of the stationary random process must satisfy for the autocorrelation ergodic theorem is the autocorrelation ergodic function Er(A):

$$\mathrm{Er}(A)=\lim_{T\to\infty}\frac{1}{T}\int_0^{2T}\left(1-\frac{\tau'}{2T}\right)\left[B(\tau')-\left|R_A(\tau)\right|^2\right]d\tau'=0; \tag{6a}$$

$$B(\tau')=E\left\{A(t+\tau+\tau')\,A(t+\tau')\left[A(t+\tau)\,A(t)\right]\right\}. \tag{6b}$$

where $B(\tau')$ is the temporal fourth-order moment of variable A. Autocorrelation ergodic function Er(A) is the time integral of variance between the temporal fourth-order moment $B(\tau')$ of variable A and autocorrelation function $R_A(\tau)$. If the autocorrelation ergodic function Er(A) converges to zero, then the stationary random process will be of autocorrelation ergodicity, and thus the autocorrelation ergodicity means that the fourth-order moment of the variable of the stationary random process will converge to the square of its autocorrelation function $R_A(\tau)$. Equation (6a) is the autocorrelation ergodic theorem. The autocorrelation ergodic function of the corresponding discrete variable can be determined as follows:

$$\mathrm{Er}(A)=\lim_{n\to\infty}\sum_{i=0}^{n}\left(1-\frac{\tau_i'}{n}\right)\left[B(\tau_i')-\left|R_A(\tau_j)\right|^2\right]=0, \tag{7a}$$

$$B(\tau'_i) = E\left\{\sum_{j=0}^{n} A(t+\tau_j+\tau'_i)\,A(t+\tau'_i)\left[A(t+\tau_j)\,A(t)\right]\right\}. \quad (7b)$$

Equation (7a) is the ergodic theorem of the autocorrelation function of the discrete variable. Hence, Eqs. (6a) and (7a) can also be used as the basis to test the autocorrelation ergodicity.

The stationary random process conforms to Eqs. (4) and (5), viz. it satisfies the average ergodic theorem, or that the random process is of average ergodicity; if the stationary random process conforms to Eqs. (6a) and (7a), then it satisfies the autocorrelation ergodic theorem, or the random process is of autocorrelation ergodicity. If the stationary random process is only of average ergodicity, then it is a strict ergodic stationary random process or narrow ergodic stationary random process. If the stationary random process is of both average ergodicity and autocorrelation ergodicity, then it is a wide ergodic stationary random process. It is thus clear that the ergodic random process is stationary, but the stationary process may not be ergodic.

With respect to the random process theory, when its average and autocorrelation function are calculated, a large amount of repeated observations of the random process is required to determine sample function $A_k(t)$. If it is a stationary random process and satisfies the ergodic conditions, then the time average of a sample on the whole time shaft can be used to substitute for the overall or ensemble average. The conditions of Eqs. (4), (5), (6a) and (7a) can be used as the basis to judge whether or not the random variable satisfies the average and autocorrelation ergodicity. The ergodic random process must be stationary, and the stationary random process is defined as Eq. (1), and thus the random process is stationary in relaxation time τ. If conditions such as Eqs (4) and (5) of the average ergodicity are satisfied, then a time average in finite relaxation time τ can be used to substitute for the infinite time average to calculate average Eq. (2) of the random variable; similarly, the finite time average can be used for substitution to calculate the covariance or variance of random variable (Eq. (3)) if conditions such as Eqs. (6a) and (7a) of the autocorrelation ergodicity are satisfied. In a similar manner, the basic principle of the turbulence measurement average is the ensemble average of space, time and state, and it is necessary to conduct mass observation for a long period of time in the whole space. This observation requires a very large investment and is hardly feasible. If the turbulence signal satisfies the ergodic conditions, the time average in relaxation time τ

by multi-station observation, and even single-station observation, can be used to substitute for the ensemble average. In fact, the precondition to estimate the turbulent features (including turbulent flux) by the eddy correlation method is that the turbulence satisfies the ergodic conditions. Therefore, conditions such as Eqs. (4), (5), (6a) and (7a) will also be the basis for testing the authenticity of the observed results by the eddy correlation method.

2.2 Band-pass filtering

The turbulence in the atmospheric boundary layer is wide in scale. A major goal of our study is to understand what type of eddy in the scale can satisfy the ergodic conditions. Another goal is to use the time average of the signal measured by a single station for the accurate measurement of the turbulent features. In order to study the ergodicity of the eddies in different scales, Fourier transform was used as band-pass filtering to separate the eddies in different scales. That is to say, we set the frequency spectrum to be removed when filtering to zero in the Fourier transform, then determined the signal after filtering by means of Fourier inverse transformation. The specific formula is shown below:

$$F_A(n)=\frac{1}{N}\sum_{k=0}^{N-1}A(k)\cos\left(\frac{2\pi nk}{N}\right)-\frac{i}{N}\sum_{k=0}^{N-1}A(k)\sin\left(\frac{2\pi nk}{N}\right), \tag{8}$$

$$A(k)=\sum_{n=a}^{N-1}F_A(n)\cos\left(\frac{2\pi nk}{N}\right)+i^2\sum_{n=a}^{N-1}F_A(n)\sin\left(\frac{2\pi nk}{N}\right). \tag{9}$$

In Eqs. (8) and (9), $A(k)$ indicates N data points from k=0 to k=N-1, and n is the cycle index of the observation time range. Through high-pass filtering (a is the lower limit wave-number of filtering) it is possible to cut off the low frequency turbulence and obtain a high frequency turbulence signal. Although the aliasing of a half high frequency turbulence after the Fourier transformation cannot be avoided, the correction for high frequency response will compensate for the loss. In order to acquire a purely high frequency signal, the band-pass filtering results from n=j to n=N-j of the high frequency signal were obtained in the filtering process. This is referred to as j time filtering in this paper. Finally, the ergodicity of the eddies in the different scales was analyzed using Eqs. (4)-(6).

2.3 M-O similarity of turbulence variance

The M-O similarity relations of the turbulence variance can be regarded as an effective measure to verify whether or not the turbulent flow field is steady and

286 homogeneous (Foken et al. 2004). Under ideal conditions, the local M-O similarity
287 relations of variance of wind velocity, temperature and other factors can be expressed
288 as follows:

289 $$\sigma_i / u_* = \phi_i(z/L), \qquad (i = \boldsymbol{u}, \boldsymbol{v}, \boldsymbol{w}), \tag{10}$$

290 $$\sigma_s / |s_*| = \phi_s(z/L), \quad (s = \theta, q, \rho_c). \tag{11}$$

291 where σ is the turbulence variance; corner mark i is the wind velocity $\boldsymbol{u}$, $\boldsymbol{v}$ or $\boldsymbol{w}$; s
292 stands for scalar, such as potential temperature θ, humidity q and CO_2 concentration ρ_c;
293 u_* is the friction velocity and defined as $u_* = \left(\overline{\boldsymbol{u}'\boldsymbol{w}'}^2 + \overline{\boldsymbol{v}'\boldsymbol{w}'}^2\right)^{1/4}$; s_* is the turbulent
294 feature of the related scalar and is defined as $s_* = -\overline{\boldsymbol{w}'s'}/u_*$; and M-O length L is
295 defined as shown below:

296 $$L = u_*^2 \theta / [\kappa g(\theta_* + 0.61\theta q_* / \rho_d)]. \tag{12}$$

297 A large number of research results show that, in the case of unstable stratification,
298 $\phi_i(z/L)$ and $\phi_s(z/L)$ can be expressed in the following forms (Panofsky et al. 1977;
299 Padro 1993; Katul et al. 1999), under ideal conditions:

300 $$\phi_i(z/L) = c_1(1 - c_2\, z/L)^{1/3}; \tag{13}$$

301 $$\phi_s(z/L) = \alpha_s(1 - \beta_s\, z/L)^{-1/3}. \tag{14}$$

302 where c_1, c_2, α and β are the undetermined coefficients. In the case of stable
303 stratification, $\phi_s(z/L)$ is approximate to the constant and $\phi_i(z/L)$ is still the 1/3
304 function of z/L. The turbulence characteristics of the eddies in the different temporal
305 and spatial scales in the atmosphere are compared and analyzed with Eqs. (13) and
306 (14), to test the feasibility of the M-O similarity under conditions of the ergodic and
307 non-ergodic turbulence.

308 **3 Observation site and data processing**

309 Two sets of data were used in the study. The first included the atmospheric surface
310 layer data measured by a 10 Hz 3-D ultrasonic wind and temperature tester (CSAT3)
311 and infrared gas analyzer (Li7500) at the Nagqu Station of Plateau Climate and
312 Environment, Chinese Academy of Sciences, from 23 July 2011 to 13 September
313 2011. The second data set was collected from the 20 Hz atmospheric surface layer at
314 seven observation points (CASES-99) in the Kansas prairies (Poulos et al. 2002;

315 Chang et al. 2002). The two sets of data, collected for completely different purposes,
316 were compared to test the universality of the research results. The geographic
317 coordinate of Nagqu Station is 31.37°N, 91.90°E, and its altitude is 4509 m a.s.l. The
318 observation station is built on flat and wide area except for a hill of about 200 m at 2
319 km distance in the north, the ground surface is mainly composed of sandy soil mixed
320 with some fine stones, and an alpine meadow with vegetation of 10-20 cm in height
321 grows in the area (see Fig. 1a). The CASES-99 data used included the data measured
322 by a 10 m high 3-D wind and temperature tester (ATI) on the central tower (37.65°N,
323 96.74°W) of 55 m height; and other turbulence data were measured by a 10 m high
324 3-D ultrasonic wind velocity system (ATI) and infrared gas analyzer (Li7500) on six
325 small towers surrounding the main tower. The small towers, sn1, sn2 and sn3 were
326 located 100 m away from the main tower, the sn4 was 280 m away, and tower sn5 and
327 sn6 were located 300 m away. The specific positions were as shown in Fig. 1(b).
328 Similar to Nagqu Station, the CASES-99 observation field was flat and there were
329 grasses of 20-50 cm in height present during the test period. The displacement height
330 of the underlying surface of the Nagqu meadow was determined to 0.03 m by
331 calculation, while the displacement height of the CASES-99 underlying surface was
332 0.06 m (Martano 2002).
333 This study is conditioned to the stationary random process. So the inaccurate data in
334 the measurements caused by circuit were deleted before data analysis. Subsequently,
335 the collected data were divides into continuous sections of 5-hour, and the 1-hour high
336 frequency signals were obtained by applying Eqs. (8) and (9) on each 5-hour data. In
337 order to conform to the stationary random condition and to select the steady turbulent
338 data, the 12 fragments of 5-min velocity and temperature variances in 1-hour were
339 calculated and compared with each other. When their deviations were less than
340 $\pm 15\%$ (including an instrumental error of about $\pm 5\%$), the data were selected to
341 study the ergodicity of the observed eddies. In addition, ultrasonic temperature pulse
342 was corrected to absolute temperature pulse (Schotanus et al. 1983; Kaimal et al.
343 1991). Then the coordinate was rotated using the plane fitting method to improve the
344 installation level (Wilczak 2001). In the view that moisture and CO_2 were components
345 of the air, their pulsation was also a constituent part of the air density pulsation.
346 Therefore, there was no related correction on the humidity or CO_2 pulsation caused by
347 air density fluctuation. In addition, according to our preliminary analysis, such

correlation may also cause the results to unreasonably deviate from the prediction shown in Eq. (14). The Webb correction (Webb et al. 1980) is the component of the surface energy balance in physical nature, but not the component of the turbulent eddy. We thus did not perform Webb correction on our research objectives of the ergodicity of the eddies in the different scales.

4. Result analysis

4.1 Verification of average ergodic theorem of eddies in different temporal scales

Applying the two sets of data from Nagqu Station and CASES-99, we had tested the average ergodicity of the eddies in different temporal scales under the condition of stationary random and steady turbulence. Here, we carefully select the representative data measured at the Nagqu Station at the height of 3.08 m during three time frames, namely 3:00-4:00, 7:00-8:00 and 13:00-14:00 China Standard Time on 25 August, in clear weather, as the case to test and demonstrate the average ergodicity of the eddies in different temporal scales. These three time frames can represent three situations, namely the nocturnal stable boundary layer, early neutral boundary layer and midday convective boundary layer. It is noted that the data were not filtered when calculating the stratification stability, since the signal of whole turbulence were needed. The stratified stability is 0.02, -0.004 and -0.54 for 3:00-4:00, 7:00-8:00 and 13:00-14:00, respectively.

The trend correction (McMillen 1988; Moore 1986) of the data measured in the eddy correlation method has been widely accepted. In nature, this is a type of high-pass filtering which is used to exclude the influence of the low frequency effect of temperature and other diurnal variation on turbulent flux. In order to acquire the effective information of the eddies in the different temporal scales, first Eqs. (8) and (9) were used to perform band-pass filtering of the Nagqu 3.08 m turbulence data, which was equivalent to the correction of the high-pass filtering. In addition, the results of the time band-pass filtering from $n=j$ to $n=N-j$ corresponding to Eqs. (8) and (9) indicated the information of the eddy in the corresponding temporal scale. The band-pass filtering information of the different time frames was thereby utilized to study the turbulence characteristics and the ergodicity of the eddies in the different temporal scales of the six time frames, including 2 min, 3 min, 5 min, 10 min, 30 min and 60 min.

The M-O stratification stability z/L describe a whole characteristic between the

mechanical and buoyancy effects in turbulence, but this study will decompose the turbulence into the different scale eddies. Considering that the features of the different scale eddies of atmospheric turbulence varied with the atmospheric stability parameter z/L, a local M-O stratification stability parameter that was limited in the certain scale range of eddies was defined as $(z\text{-}d)/L_c$, so as to analyze the relationship between the stratification stability and average ergodicity of the wind velocity, temperature and other factors of the eddies in the different scales. It is noted that the local stability is different from the M-O stratification stability $(z\text{-}d)/L$.

We took the local stability of the eddies in the different temporal scales of the three time frames from nighttime to daytime as an example, as shown in Table 1.

The results show that the local stability parameter $(z\text{-}d)/L_c$ of eddy below 2 min in temporal scale during the time frame of 3:00-4:00 (nighttime) was 0.59, thus it was stable stratification. For the eddy of which the temporal scale gradually increased from 3 min, 5 min and 10 min to 60 min, the $(z\text{-}d)/L_c$ also gradually decreased to 0.31 and 0.28. In addition, beginning from the eddy of 10 min in the temporal scale, even the local stability decreased, namely from -0.01 to -0.07. It seemed that the local stability gradually varied from stability to instability as the temporal scale of eddy increased. During the time frame of 7:00-8:00 (morning), the $(z\text{-}d)/L_c$ of the eddies from 2 min to 60 min in the temporal scale eventually decreased from 0.52, 0.38, 0.16 and 0.15 to a minimum of -1.29, which meant that the eddy in the temporal scales of 30 min and 60 min had high local instability. However, during the time frame of 14:00-15:00 (midday), the $(z\text{-}d)/L_c$ of the eddy from 2 min to 60 min in the temporal scale was unstable. As the scale of the eddy increased, the local instability of the eddies on the scale from 2 min to 3 min also increased, and the instability value reached the maximum of 0.44 when the scale of the eddy was 5 min; the scale of the eddy continuously increased, but the local instability of the eddy decreased.

The M-O local stability of an eddy is not entirely the same as the M-O stratification stability of the boundary layer in terms of physical significance, and the M-O stratification stability of the boundary layer indicates that the overall effect of the atmospheric stratification in the boundary layer on the stability of all eddies in integral effect. The local stability of the eddy is only a local effect of the atmospheric stratification on the stability of the eddy in a certain scale. As the scale of the eddy increases, the local stability of the eddy will vary accordingly. The aforesaid results

indicate that the local stability of small-scale eddies was stable in the nocturnal stable boundary layer, but the nocturnal stable boundary layer was possibly unstable for the large-scale eddies, so as to result in a sink effect on the small-scale eddies but a buoyancy effect on the large-scale eddies. However, in the diurnal unstable boundary layer, the local stability of the eddy of 3 min in scale reached the maximum, the instability of the smaller eddies decreased, but the instability gradually decreased as the scale of the eddy increased. Therefore, the eddy of 3 min in the scale bore maximum buoyancy, but the buoyancy of the eddy decreased as the scale of the eddy increased. In addition, the small-scale eddies were more stable than the eddies in the large scale in the nocturnal stable boundary layer; while the large-scale eddies were more stable than the eddies in the small scales in the diurnal unstable and convective boundary layers. The above observations signify that it is common for the-small scale eddies to exist in the nocturnal stable boundary layer, and it is also common for the large-scale eddies to exist in the diurnal convective boundary layer. Therefore, it is clear that the small-scale eddies are dominant in the nocturnal stable boundary layer, while the large-scale eddies are dominant in the diurnal convective boundary layer.

Finally, we calculated the autocorrelation function of the eddies in the different temporal scales using Eq. (5), as well as the variation of the average ergodic function Ero(A) with relaxation time τ if relaxation time $\tau_{i=n}$ was cut off, and verified the ergodic theorem of average value. The average ergodic function Ero(A) of the vertical velocity, temperature and specific humidity of the eddies in the different scales of the three time frames of 3:00-4:00, 7:00-8:00 and 13:00-14:00 China Standard Time were measured at the Nagqu Station at the height of 3.08 m, and varied with relaxation time τ, as shown in Figs. 2-4a, b and c, respectively. To facilitate comparison, Fig. 5 shows the variation of the average ergodic function Ero(A) of vertical velocity (a), temperature (b) and specific humidity (c) before filtering during the time frame of 14:00-15:00 (midday) with relaxation time τ. Since the ergodic function varied within a large range, the ergodic functions were normalized according to the features of their variables ($A_* = \boldsymbol{u}_*, |\theta_*|, |q_*|$). That is to say, the functions in the following figures are dimensionless ergodic functions, Ero(A)/A_*.

The characteristics of the average ergodicity of turbulence, as well as comprehensive analysis on related causes, are as follows:

1. Verifying average ergodic theorem of eddies in different scales: according to the

447 average ergodic theorem of eddies, Eq. (4), the average ergodic function
448 Ero(A)/A_* will converge to 0 when the time approaches infinite. This is a
449 theoretical result of the stationary random process. However, the calculated
450 average ergodic function was obtained under the condition that relaxation time
451 $\tau_{i=n}$ was cut off. If the average ergodic function Ero(A)/A_* is approximately 0 in
452 relaxation time $\tau_{i=n,}$ it will be considered that A approximately satisfies the
453 average ergodic theorem; if the average ergodic function deviates more from zero,
454 the average ergodicity will be far lower, so as to approximately determine
455 whether or not the average ergodic theorem of the eddies in different scales is
456 established. Figures. 2-4 clearly show that, regardless of vertical velocity,
457 temperature or humidity, the Ero(A)/A_* of eddies below 10 min in the temporal
458 scale will fluctuate around zero within a small range; thus we may conclude that
459 the average ergodic function Ero(A)/A_* of the eddy below 10 min in the temporal
460 scale converges to zero and can effectively satisfy the conditions of the average
461 ergodic theorem. For the eddies of 30 min and 60 min, if the eddy is larger in
462 scale, then the average ergodic function Ero(A)/A_* will derivate further from zero.
463 In particular, the average ergodic function Ero(A)/A_* of the eddies of 30 min and
464 60 min of the temperature or humidity does not converge, and even diverges. The
465 above results show that the average ergodic function of the eddies of 30 min and
466 60 min cannot converge to zero or satisfy the conditions of the average ergodic
467 theorem.
468 2. Comparison of the convergence of the average ergodic function of vertical
469 velocity, temperature and humidity: as seen from Figs. 2-4, if the dimensionless
470 average ergodic function of the vertical velocity is compared with the function
471 value of the temperature or humidity, it is 3-4 magnitudes less than those in the
472 nocturnal stable boundary layer; 1-2 magnitudes less than those in the early
473 neutral boundary layer; and around 2 magnitudes less than those in the midday
474 convective boundary layer. For example, during the time frame of 3:00-4:00
475 (nighttime), the dimensionless average ergodic function of the vertical velocity is
476 10^{-5} in magnitude, while the respective magnitudes of the function value of the
477 temperature and humidity are 10^{-1} and 10^{-2}; during the time frame of 7:00-8:00
478 (morning), the magnitude of the dimensionless average ergodic function of the
479 vertical velocity is 10^{-4}, while the respective magnitudes of the function value of

the temperature and humidity are 10^{-2} and 10^{-3}; during the time frame of 13:00-14:00 (midday), the magnitude of the dimensionless average ergodic function of the vertical velocity is 10^{-4}, while the magnitudes of the function values of the temperature and humidity are both 10^{-2}. These results show that the dimensionless average ergodic function of the vertical velocity converges to zero more frequently than the function value of the temperature and humidity, and that the vertical velocity satisfies the conditions of the average ergodic theorem more easily than the temperature and humidity.

3. Temporal scale and spatial scale of turbulent eddy: for wind velocity of 1-2 ms^{-1}, the spatial scale of the eddy of 2 min in the temporal scale is around 120-240 m, and the spatial scale of the eddy of 10 min in the temporal scale is around 600-1200 m. The spatial scale of the eddy of 2 min in the temporal scale is equivalent to the height of the surface layer, and the special scale of the eddy of 10 min in the temporal scale is equivalent to the height of the atmospheric boundary layer. The spatial space of the eddy within 30-60 min in the temporal scale is around 1800-3600 m, and this spatial scale clearly exceeds the height of the atmospheric boundary layer. According to stationary random process definition (1) and the average ergodic theorem, the stationary random process must be stable in relaxation time τ. The eddy below 10 min in the temporal scale in the height of the atmospheric boundary layer is a stationary random process, and can effectively satisfy the conditions of the average ergodic theorem. However, the eddies of 30 min and 60 min in the temporal scale exceed the height of the atmospheric boundary layer and do not satisfy the conditions of the average ergodic theorem, thus these eddies belongs to the nonstationary random process.
4. Ergodicity of turbulence of all eddies in the possible scales of the atmospheric boundary layer: Fig. 5 shows the unfiltered average ergodic function of the eddies in possible scales in the atmospheric boundary layer. When Fig. 5 is compared with Figs. 2c, 3c and 4c, for the turbulence of all eddies in possible scales in the boundary layer, during the time frame of 14:00-15:00 (midday), the average ergodic function $\mathrm{Ero}(A)/A_*$ of the vertical velocity, temperature and humidity of the convective boundary layer before filtering is greater than the average ergodic function of the turbulence of the eddies in the different scales

after filtering. As shown in Figs. 2c, 3c and 4c, the magnitude of the vertical velocity is 10^{-4} and the magnitudes of the temperature and specific humidity are both 10^{-2}; according to Fig. 5, the magnitude of the vertical velocity Ero(A)/A_* is 10^{-3} and the magnitudes of the temperature and specific humidity are both 10^{0}, therefore 1-2 magnitudes are almost improved. In addition, all trend upward (vertical velocity and temperature) or downward (specific humidity), deviating from zero. It is thus clear that, even if the time of day is 14:00-15:00, the average ergodic function of all eddies in the possible scales in the convective boundary layer cannot converge to zero before filtering, and thus local circulation in convective boundary layer cannot satisfy the conditions of the average ergodic theorem. We argue that, under general conditions, the eddy below 10 min in the temporal scale or within 600-1200 m in the spatial scale within the height of the atmospheric boundary layer is the ergodic stationary random process, and the turbulence of the eddies in all possible scales including the boundary layer may belong to the non-ergodic stationary random process.

5. Relation between ergodicity and local stability of eddies in different scales: the corresponding local stability parameters (z-d)/L_c of eddies at different times in different scales (see Table 1) show that the local stability parameters (z-d)/L_c of the eddies in the different scales are different, due to the fact that the temperature stratification in the atmospheric boundary layer has different effects on the stabilities of the eddies in the different scales. Entirely different results can occur, and the stratification which can cause the eddies in the large scale to rise may cause the eddies in the small scale to descend at the same time. However, the analysis results in Figs. 2-4 show that the ergodicity is mainly related to the eddy scale, and its relation with the atmospheric temperature stratification is not significant.

4.2 Verification of autocorrelation ergodic theorem for eddies in different scales

In the following section, Eqs. (7a) and (7b) are used to verify the autocorrelation ergodic theorem. It was identified in Sect. 4.1 that the turbulent eddies below 10 min in the temporal scale satisfy the average ergodic conditions in the various time frames, i.e., the turbulent eddies below 10 min in the temporal scale are at least in strictly stationary random processes or narrow stationary random processes in the nocturnal stable boundary layer, early neutral boundary layer and midday convective boundary

546 layer. Then these eddies are used to further analyze whether or not the turbulent
547 eddies in the different scales which satisfy the average ergodic conditions also satisfy
548 the autocorrelation ergodic conditions, so as to verify whether atmospheric turbulence
549 is in the narrow stationary random process or wide ergodic stationary random process.
550 The ergodic theorem of the autocorrelation function of the turbulence variable under
551 the condition of truncated relaxation time $\tau_{i=n}$ were calculated according to Eq. (7a) to
552 determine the variation of the ergodic theorem of autocorrelation function Er(A) with
553 relaxation time τ. As with the average ergodic function Ero(A), if the ergodic theorem
554 of the autocorrelation function Er(A) of the eddies of 2 min, 3 min, 5 min, 10 min, 30
555 min and 60 min in the temporal scale within the relaxation time $\tau_{i=n}$ is approximate to
556 0, then A shall be deemed to be approximately ergodic; the more the ergodic theorem
557 of the autocorrelation function deviates from 0, the worse the autocorrelation
558 ergodicity becomes. Therefore, this method should be used for approximating
559 whether eddies in the different scales satisfy the conditions of the autocorrelation
560 ergodic theorem or the ergodicity.

561 For example, Fig. 6 shows the variation of the ergodic theorem of normalized
562 autocorrelation function Ero($\boldsymbol{w}$)/u_* of the turbulent eddies of 2 min, 3 min, 5 min, 10
563 min, 30 min and 60 min in the temporal scale of vertical velocity during the time
564 frames of 3:00-4:00, 7:00-8:00 and 13:00-14:00 with relaxation time τ. Some basic
565 conclusions are drawn from Fig. 6:

566 1. After comparing Figs. 6a-c with Figs. 2a-c, the dimensionless average ergodic
567 function Ero($\boldsymbol{w}$)/u_* of the vertical velocity with the dimensionless ergodic
568 theorem of autocorrelation function Er($\boldsymbol{w}$)/u_* of the vertical velocity, two basic
569 characteristics are very clear. First, the magnitudes of the dimensionless ergodic
570 theorem of autocorrelation function Er($\boldsymbol{w}$)/u_*, regardless of whether in the
571 nocturnal stable boundary layer, early neutral boundary layer or midday
572 convective boundary layer, are all greatly reduced. In Figs. 2a-c, the magnitudes
573 of Ero($\boldsymbol{w}$)/u_* are respectively 10^{-5}, 10^{-4} and 10^{-4}, and the magnitudes of Er($\boldsymbol{w}$)/u_*
574 are respectively 10^{-7}, 10^{-5} and 10^{-5}, as shown in Figs. 6a-c. The magnitudes of
575 Er($\boldsymbol{w}$)/u_* reduce by 1-2 compared with those of Ero($\boldsymbol{w}$) /u_*. Second, all ergodic
576 theorem of autocorrelation functions Er($\boldsymbol{w}$)/u_* of the eddies of 30 min and 60 min
577 in the temporal scale, regardless of whether they are in the stable boundary layer,
578 natural boundary layer or convective boundary layer, are all reduced and

579 approximate to Ero ($\boldsymbol{w}$)/u_* of the eddy below 10 min in the temporal scale.
580 2. The above two basic characteristics imply that the ergodic theorem of the
581 autocorrelation function Er($\boldsymbol{w}$)/u_* of the stable boundary layer, neutral boundary
582 layer or convective boundary layer converges to 0 faster than the average ergodic
583 function Ero ($\boldsymbol{w}$)/u_*; the ergodic theorem of the autocorrelation function of the
584 eddies of 30 min and 60 min in the temporal scale also converge to 0 and satisfy
585 the conditions of the autocorrelation ergodic theorem, except for the fact that the
586 ergodic theorem of autocorrelation function Er($\boldsymbol{w}$)/u_* of the eddy below 10 min in
587 the temporal scale can converge to 0 and satisfy the conditions of the
588 autocorrelation ergodic theorem.
589 3. According to the ergodic theorem of the autocorrelation function, both eddies of
590 30 min and 60 min and the eddy below 10 min in the temporal scale, regardless
591 of whether they are in the stable boundary layer, neutral boundary layer or
592 convective boundary layer, can satisfy the conditions of the ergodic theorem of
593 autocorrelation function Eq. (7a), i.e., they can satisfy the conditions of the
594 ergodic theorem. Therefore, in general the turbulence in the atmospheric
595 boundary layer is the autocorrelation ergodic stationary random process.
596 4. The above observation results show that the eddies below 10 min in the temporal
597 scale in the nocturnal stable boundary layer, early neutral boundary layer and
598 midday convective boundary layer can not only satisfy the conditions of the
599 average ergodic theorem, but they can also satisfy the conditions of the
600 autocorrelation ergodic theorem. Therefore, the eddies below 10 min in the
601 temporal scale are wide ergodic stationary random processes. Although the
602 eddies of 30 min and 60 min in the temporal scale in the stable boundary layer,
603 neutral boundary layer and convective boundary layer can satisfy the conditions
604 of the autocorrelation ergodic theorem, they cannot satisfy the conditions of the
605 average ergodic theorem. Therefore, the eddies of 30 min and 60 min in the
606 temporal scale are neither ergodic narrow stationary random processes, nor wide
607 ergodic stationary random processes.

608 **4.3 Verification of ergodic theorem of eddies in different scales measured by**
609 **multiple stations**

610 The basic principle of the turbulence measurement average is the ensemble average of
611 space, time and state. Sections 4.1 and 4.2 verify the average ergodic theorem and

ergodic theorem of the autocorrelation function of the atmospheric turbulence during the stationary random process using observation data, so that the finite time average of a single station is used to substitute for the ensemble average. This section examines the ergodicity of the eddies in different scales according to the observational data collected at the CASES-99 tower and six observation sites (seven stations). When the data were selected, it was considered that if the eddy was not evenly distributed at the seven stations, then the observation results at the seven stations may have originated from many eddies in a large scale. For this reason, we first compared the high frequency variance spectrum above 0.1 Hz. Based on the observational error, if the difference of all high frequency variances does not exceed the average by ±10%, then it is assumed that the turbulence is evenly distributed at the seven observation stations. Finally, 17 datasets were collected from among the turbulence observation data from 5 to 30 October, and these data sets refer to the results of strong turbulence at noon on a sunny day. As an example, the same method as described in Sections 4.1 and 4.2 is used to respectively calculate the variation of the average ergodic function and ergodic theorem of the autocorrelation function of the vertical velocity at 10:00-11:00 on 7 October with relaxation time τ. Next, the observation data collected from the seven stations are built into a data set, and the time series of the data set are filtered at 2 min, 3 min, 5 min, 10 min, 30 min and 60 min, the variation of the average ergodic function $\mathrm{Ero}(\boldsymbol{w})/u_*$ and ergodic theorem of the autocorrelation function $\mathrm{Ero}(\boldsymbol{w})/u_*$ of the vertical velocity with relaxation time τ is analyzed to test the ergodicity of eddies in the different scales in the multi-station observation data. Figure 7a shows the variation of the average ergodic function $\mathrm{Ero}(\boldsymbol{w})/u_*$ of the vertical velocity with relaxation time τ, and Fig. 7b shows the variation of the ergodic theorem of the autocorrelation function $\mathrm{Ero}(\boldsymbol{w})/u_*$ with relaxation time τ. The results are as follows:

1. Ergodic characteristics of the eddies in the different scales measured at the multi-stations: Fig. 7a shows that the average ergodic function of the eddies below 30 min in the temporal scale converges to 0 very well, except for the fact that the average ergodic function of eddy of 60 min in the temporal scale clearly deviates upward from 0. Fig. 7b shows that all ergodic theorems of the autocorrelation functions of the eddies in the different scales, including the eddy of 60 min in the temporal scale, gradually converge to 0. Therefore, the eddies

below 30 min in the temporal scale measured at the multi-stations satisfy the conditions of both the average and autocorrelation ergodic theorems, while the eddy of 60 min in the temporal scale only satisfies the conditions of autocorrelation ergodic theorem, but cannot satisfy the conditions of the average ergodic theorem. These observations demonstrate that the eddies below 30 min in the temporal scale are wide ergodic stationary random processes in the data series composed of observation data collected from the seven stations. This signifies that the temporal scale of the eddy during the wide ergodic stationary random process has extended from below 10 min to 30 min in the data series composed of observation data collected from multiple stations, compared with the observation data collected from a single station. As analyzed above, if the eddy below 10 min in the temporal scale is deemed to be a turbulent eddy in the 1000 m boundary layer and the eddy of 30 min in the temporal scale is deemed to be a local circulated eddy in the greater than 2000 m boundary layer, then multiple station observations can completely capture the local circulated eddy of 30 min in the temporal scale in the boundary layer.

2. Average time problem of turbulent feature average: according to the average ergodic theorem, if the condition of average ergodic theorems Eqs. (4) or (5) is satisfied, then a time average of finite relaxation time τ is used to substitute for the average of the infinite time and calculate the average random variable Eq. (2). This signifies that the calculation of the turbulence average is restricted not only by the average ergodic theorem, but also is closely related to the scale of the turbulent eddy. The analysis on the ergodicity of eddies in the different scales in the above two sections demonstrates that the eddies below 10 min in temporal scale at τ=30 min in the stable boundary layer, neutral boundary layer and convective boundary layer can not only satisfy the conditions of the average ergodic theorem, but can also satisfy the conditions of the autocorrelation ergodic theorem. That is to say, they are namely wide ergodic stationary random processes. Therefore, the finite time average of 30 min within relaxation time τ can be used for substituting for the ensemble average to calculate average random variable Eq. (2). However, the eddies of 30 min and 60 min in the temporal scale in the stable boundary layer and neutral boundary layer are only autocorrelation ergodic random processes, rather than narrow and wide sense

random processes. Therefore, when the finite time average of 30 min can be used for substituting for the ensemble average to calculate average random variable Eq. (2), it may capture the stationary random processes of the eddy below 10 min in the temporal scale, but not completely capture the nonstationary random process of the eddies above 30 min in the temporal scale. In the observation performed using the eddy correlation method, the substitution of the ensemble average with finite time average of 30 min inevitably results in a high level of error, due to lack of low frequency component information of the large-scale eddy. However, although the eddies of 30 min and 60 min in the temporal scale in the convective boundary layer are not wide ergodic stationary random processes, they are autocorrelation ergodic random processes. This may imply that the average random variable which is calculated with the finite time average in the convective boundary layer to substitute for the ensemble average is often superior to the results of the stable boundary layer and neutral boundary layer. In addition, the results in the previous sections also show that the dimensionless average ergodic function of the vertical velocity may more easily converge to 0 than the functions corresponding to the temperature and humidity, and the vertical velocity may more easily satisfy the conditions of average ergodic theorem than the temperature and humidity. Therefore, in the observation performed using the eddy correlation method, the results of the vertical velocity are often superior to those of the temperature and humidity. In this section, the results also point out that multi-station observation is capable of completely capturing the eddy of local circumfluence in the local boundary layer. Therefore, ergodic assumption is more likely to be satisfied, and its results are much closer to the true values when calculating the turbulence average, variance or turbulent flux with the multi-station observation data.

4.4 M-O similarity of turbulent eddies in different scales and its relation with ergodicity

Turbulent variance is the most basic turbulent feature. Turbulence velocity variance, which represents turbulence intensity, and the variance of scalars, such as temperature and humidity, effectively describes the structural characteristics of turbulence. In order to test the relation of the M-O similarity of the turbulent eddies in the different scales with ergodicity, and take it as an example of the above ergodic testing, the

711 vertical velocity and temperature data of Nagqu from 23 July to 13 September are
712 used to determine the M-O similarity of the vertical velocity and temperature
713 variances for the eddies in the different scales, and analyze its relation with the
714 ergodicity.

715 Figures 8 and 9 respectively shows the similarity curves of the eddies in the
716 different scales for the vertical velocity and temperature variances in Nagqu, where
717 (a), (b) and (c) are respectively the similarity curve of eddies of 10 min, 30 min and
718 60 min in the temporal scale; Table 2 also shows the below fitting curve of the
719 similarity of the vertical velocity variance and relevant parameters:

720 $$\phi_i\left(z/L\right)=c_1\left(1-c_2\,z/L\right)^{1/3},\quad z/L<0, \tag{15}$$

721 $$\phi_i\left(z/L\right)=c_1\left(1+c_2\,z/L\right)^{1/3},\quad z/L>0. \tag{16}$$

722 The correlation coefficient and residual in the fitting curve are respectively expressed
723 with *R* and *S*.

724 Figure 8 and Table 2 show that the parameters of the fitting curve are greatly
725 different, even if the fitting curve of similarity of the vertical velocity variance for the
726 eddies in the different temporal scales is the same. The correlation coefficients of the
727 fitting curve of similarity of the vertical velocity variance at unstable stratification are
728 large, but the correlation coefficients at stable stratification are small. At unstable
729 stratification, the correlation coefficient of the eddy of 10 min in the temporal scale
730 reaches 0.97, while the residual is only 0.16; at stable stratification, the correlation
731 coefficient reduces to 0.76, but the residual increases to 0.25. With the increase of the
732 temporal scale of the eddy from 10 min (Fig. 8a) to 30 min (Fig. 8b) and 60 min (Fig.
733 8c), the correlation coefficients of similarity of the vertical velocity variance gradually
734 reduce, but the residual increases. The correlation coefficient in 60 min is the
735 minimum; it is only 0.83 at unstable stratification, and only 0.30 at stable
736 stratification.

737 The temperature variance is shown in Fig. 9. The below function is fitted from the
738 eddy of 10 min in the temporal scale at unstable stratification:

739 $$\phi_\theta\left(z/L_c\right)=4.9\left(1-79.7\,z/L_c\right)^{-1/3}. \tag{17}$$

740 As shown in Fig. 9a, the correlation coefficient of the fitting curve is -0.91 and
741 residual is 0.38. With the increase of the temporal scale of the eddy, the discreteness
742 of similarity of the temperature variance is enlarged quickly, and an appropriate curve

is not fitted.

The above results show that the discreteness of similarity of the turbulence variance is enlarged with the increase of temporal scale of the eddy for either the vertical velocity or temperature. The data points collected during the stationary process basically gather near the fitting curve of the variance similarity, while all data points during the nonstationary process deviate significantly from the fitting curve. However, the similarity of the vertical velocity variance is superior to the similarity of the temperature variance. These observations are the same as the testing conclusions of ergodicity for the eddies in the different scales described in Sections 4.1-4.3. The ergodicity of the small-scale eddy is superior to that of the larger-scale eddy, and the eddy of 10 min in the temporal scale has the best variance similarity function. These observations also signify that when the eddy at the stationary random process satisfies the ergodic conditions, then both the vertical velocity variance and temperature variance of the eddies in the different temporal scales comply with the M-O similarity theory very well; but, as for the eddy during nonstationary random process or with poor ergodicity, the eddy variance deviates from the M-O similarity relation.

5 Discussion

The turbulence in the atmospheric boundary layer is a eddy structure; when the temporal scale of the turbulent eddy in the atmosphere surface layer is about 2 min, the corresponding spatial scale is about 120-240 m; when the temporal scale of the turbulent eddy in the atmospheric boundary layer is about 10 min, the corresponding spatial scale is about 600-1200 m. As for the eddies in the larger temporal and spatial scale, such as the eddies of 30-60 min in the temporal scale, and the corresponding spatial scale is about 1800-3600 m. Spatial scale exceeds the height of the atmospheric boundary layer. As for the atmospheric turbulent eddy below the scale of the atmospheric boundary layer, i.e. the eddy below 1000 m in the spatial scale and below 10 min in the temporal scale, its average ergodic function Ero(A) and ergodic theorem of autocorrelation function Er(A) converge to 0, and they can satisfy the conditions of the average ergodic theorem and autocorrelation ergodic theorem. However, as for the atmospheric turbulent eddy above 2000-3000 m in the spatial scale and above 30-60 min in the temporal scale, its average ergodic function does not converge to 0, that is, it cannot satisfy the conditions of the average ergodic theorem. Therefore, atmospheric turbulent eddy below the scale of the atmospheric boundary

776 layer belongs to the wide ergodic stationary random process, but the atmospheric
777 turbulent eddy above the scale of the atmospheric boundary belongs to the
778 non-ergodic random process, or even the nonstationary random process. These results
779 are the success and offer a promising first step for direct evaluation of ergodic
780 hypotheses for ASL flows.

781 Galanti (2004) proved that the turbulence which was temporally steady and
782 spatially homogeneous was ergodic, but 'partially turbulent flows' such as the mixed
783 layer, wake flow, jet flow, flow around and boundary layer flow may be non-ergodic
784 turbulence. According to Galanti, it is clear that the turbulence in the atmospheric
785 boundary layer is 'partially turbulent flow', and it may be non-ergodic. However, it
786 has been proven through observational data that the ergodicity of turbulence is related
787 to the scale of the turbulent eddy. The average ergodic theorem and autocorrelation
788 ergodic theorem for the turbulent eddy in the small scale in the atmospheric boundary
789 layer is applicative, and the large-scale eddy was non-ergodic. Since the large-scale
790 eddy in the atmospheric boundary layer may be strongly influenced by the boundary
791 disturbance, it belongs to 'partial turbulence'; however, since the small-scale eddy in
792 the atmospheric turbulence may be not influenced by boundary disturbance, then it
793 belongs to the ergodic stationary process, which is temporally steady and spatially
794 homogeneous.

795 Monin-Obukhov similarity theory is used for the measurement of atmospheric
796 turbulent flux, which is developed on the conditions of steady time and homogeneous
797 surface. The homogeneous and steady conditions are in line with the ergodic
798 conditions, i.e. temporally steady and spatially homogeneously, as described by
799 Galanti. Therefore, the eddy correlation method for turbulence measurement is based
800 on the ergodic assumption and similarity theory of the atmosphere surface layer. We
801 realized from the above conclusions that the eddy in the large scale may include
802 non-ergodic random process components which exceeded the height of the
803 atmospheric boundary layer. The eddy correlation method for the measurement and
804 calculation of turbulent variance and covariance may not capture the information of
805 the large-scale eddy outside the boundary layer, thus resulting in large error.

806 **6 Conclusion**

807 The below preliminary conclusions are drawn after the ergodicity of turbulence were
808 verified by partial observational data:

1. As for the atmospheric turbulent eddy below the scale of the atmospheric boundary layer, i.e. the eddy below 1000 m in the spatial scale and below 10 min in the temporal scale, they can satisfy the conditions of the average ergodic theorem and autocorrelation ergodic theorem. However, as for the atmospheric turbulent eddy above 2000-3000 m in the spatial scale and above 30-60 min in the temporal scale, it cannot satisfy the conditions of the average ergodic theorem.
2. Although the atmospheric temperature stratification has different effects on the eddies in the different scales of stability, the ergodicity is mainly related to the local stability of the eddies, and its relation with the stratification stability of the atmospheric boundary layer is not significant.
3. When an average of finite time can be used for substituting for the ensemble average of infinite time to calculate the average random variable of the atmospheric turbulence, it may capture the stationary random process information of the eddies below 10 min in the temporal scale and below 1000 m of the atmospheric boundary layer in the spatial scale, which satisfies the conditions of the average ergodic theorem, but it does not completely capture the nonstationary random information of the turbulent eddy above 30 min in the temporal scale and above 2000 m in the spatial scale magnitude. This will inevitably cause a high level of error due to the lack of low frequency component information of the large-scale eddy when the average of finite time is used to substitute for the ensemble average in the observation using the eddy correlation method.
4. In the data set composed of observation data collected from the seven stations, the eddies below 30 min in the temporal scale belong to the wide ergodic stationary random processes. The temporal scale and spatial scale of the eddy during the wide ergodic stationary random process have extended from below 10 min to 30 min, and from below 1000 m to 2000 m in the data series composed of observation data collected from many stations, compared with the observational data collected from a single station. This signifies that the ergodic assumption is more likely to be satisfied and the observational results produced with the eddy correlation method are much closer to the true values when calculating the turbulence average, variance or turbulent flux with multi-station observation data.

5. If the stationary random process of the ergodic conditions is more effectively satisfied, then the turbulence variance of the eddies in the different temporal scales can comply with M-O similarity theory very well; however, the turbulence variance during the non-ergodic random process deviates from the M-O similarity relation.

*Acknowledgements.*This study is supported by the National Natural Science Foundation of China under Granted Nos. 91025011, 91437103 and National Program on Key Basic Research Project (2010CB951701-2). This work was strongly supported by the Heihe Upstream Watershed Ecology-Hydrology Experimental Research Station and Pingliang Station of Lightning and Hail Research, Cold and Arid Regions Environmental and Engineering Research Institute, Chinese Academy of Sciences. I would like to express my sincere regards for their support, and also thank Dr. Gordon Maclean of NCAR for providing the detailed CASES-99 data used in this study.

References

Aubinet, M., Heinesch, B., and Yernaux M.: Horizontal and vertical CO_2 advection in a sloping forest, Bound. Lay. Meteor., 108, 397-417, 2003.

Aubinet, M., Vesala, T., and Papale, D.: Eddy covariance, a practical guide to measurement and data analysis, Springer, Dordrecht, Heidelberg, London, New York, pp438, 2012.

Baldocchi, D., Finnigan, J., Wilson, K., Paw, U., and Falge, E.: On measuring net ecosystem carbon exchange over tall vegetation on complex terrain, Bound. Lay. Meteor., 96, 257-291, 2000.

Baldocchi, D., Falge, E., Gu, L., Olson, R., Hollinger, D., Running, S., Anthoni, P., Bernhofer, C., Davis, K., Evans, R., Fuentes, J., Goldstein, A., Katul, G., Law, B., Lee, X., Malhi, Y., Meyers, T., Munger, W., Oechel, W., Paw, K. T., Pilegaard, K., Schmid, H. P., Valentini, R., Verma, S., Vesala, T., Wilson, K., Wofsy, S., and Richardson, F.: FLUXNET: a new tool to study the temporal and spatial

871 variability of ecosystem-scale carbon dioxide, water vapor, and energy flux
872 densities, B. Am. Meteorol. Soc., 82, 2415–2434, 2001.
873 Birkhoff, G. D.: Proof of the ergodic theorem, Proc. Nat. Acad. Sci. USA. 18,
874 656-660, 1931.
875 Boltzmann, L.: Analytischer beweis des zweiten Haubtsatzes der mechanischen
876 Wärmetheorie aus den Sätzen über das Gleichgewicht der lebendigen Kraft, Wiener
877 Berichte , 63, 712–732, in WAI, paper 20, 1871.
878 Chang, S. S. and Huynh, G. D.: Analysis of sonic anemometer data from the
879 CASES-99 field experiment. Army Research Laboratory, Adelphi, MD. July 2002.
880 Chen, J., Fan, S., Zhao, C., Xiao, X., Cai, X. and Liu, H.: The underestimation of the
881 turbulent fluxes in eddy correlation techniques, Chinese Journal of Atmospheric
882 Sciences (in Chinese), 30(3), 423-432, 2006.
883 Chen, J., Hu Y., and Zhang L.: Principle of cross coupling between vertical heat
884 turbulent transport and vertical velocity and determination of cross coupling
885 coefficient, Adv. Atoms. Sci., 23 (4), 639-648, 2007.
886 Chen, J., Hu, Y., Lu, S., and Yu, Ye.: Experimental demonstration of the coupling
887 effect of vertical velocity on latent heat flux, Sci. China. Ser. D-Earth Sci., 56,
888 1-9, 2013.
889 Eichinger, W. E., Parlange, M. B., Katul, G. G.: Lidar measurements of the
890 dimensionless humidity gradient in the unstable atmospheric surface layer,
891 Lakshmi, V., Albertson, J. and Schaake, J., Koster, R. D., Duan, Q., Land Surface
892 Hydrology, Meteorology, and Climate, American Geophysical Union,
893 Washington, D. C. 7–13, 2001.
894 Finnigan, J. J.: A streamline coordinate system for distorted turbulent shear flows, J.
895 Fluid Mech. 130, 241–258, 1983.

896 Finnigan, J. J. and Brunet, Y.: Turbulent airflow in forests on flat and hilly terrain. In:
897 Coutts, M P, Grace J (Eds.), Wind and trees. Cambridge University Press,
898 London, 1995.
899 Finnigan, J. J.: A re-evaluation of long-term flux measurement techniques part II:
900 coordinate systems, Bound. Lay. Meteor., 113(1), 1-41, 2004.
901 Foken, T., G¨ockede, M., Mauder, M., Mahrt, L., Amiro, B. D., and Munger, J. W.:
902 Post-field data quality control, in: Handbook of micrometeorology: a guide for
903 surface flux measurement and analysis, Lee, X., Massman, W. J., and Law, B.:
904 Kluwer, Dordrecht, 181-208, 2004.
905 Foken, T., Wimmer, F., Mauder, M., Thomas, C., and Liebethal, C.: Some aspects of
906 the energy balance closure problem. Atmos. Chem. Phys., 6, 4395-4402, 2006.
907 Galanti, B. and Tsinober, A.: Is turbulence ergodic? Physics Letters A, 330, 173–18,
908 2004.
909 Geider, R. J., Delucia, E. H., Falkowski, P. G., Finzi, A. C., Grime, J. P., Grace, J.,
910 Kana, T. M., La Roche, J., Long, S. P., Osborne, B. A., Platt, T., Prentice, I. C.,
911 Raven, J. A., Schlesinger, W. H., Smetacek, V., Stuart, V., Sathyendranath, S.,
912 Thomas, R. B., Vogelmann, T. C., Williams, P. and Woodward, F. I.: Primary
913 productivity of planet earth: biological determinants and physical constraints in
914 terrestrial and aquatic habitats, Glob. Change Biol., 7(8), 849-882, 2001.
915 Higgins, C. W., Katul, G. G., Froidevaux, M., Simeonov, V. and Parlange, M. B.:
916 Atmospheric surface layer flows ergodic? Geophy. Res. Let., 40, 3342-3346,
917 2013.
918 Hu, Y.: Convergence movement influence on the turbulent transportation in
919 atmospheric boundary layer, Adv. Atoms. Sci., **20**(5), 794-798, 2003.
920 Kaimal, J. C. and Gaynor, J. E.: Another look at sonic thermometry, Bound. Lay.

921 Meteor., 56, 401–410, 1991.
922 Kaimal, J. C. and Wyngaard, J. C.: The Kansas and Minnesota experiments, Bound.
923 Lay. Meteor., 50, 31-47, 1990.
924 Katul, G. G., Hsieh, C. I.: A note on the flux-variance similarity relationships for heat
925 and water vapour in the unstable atmospheric surface layer, Bound. Lay. Meteor., 90,
926 327–338, 1999.
927 Katul, G., Cava, D., Poggi, D., Albertson, J., and Mahrt, L.: Stationarity, homogeneity,
928 and ergodicity in canopy turbulence, Handbook of micrometeorology a guide for
929 surface flux measurement and analysis, Lee, X., Kluwer Academic Publishers,
930 New York, 161−180, 2004.
931 Krengel, U.: Ergodic theorems, de Gruyter, Berlin, New York, 363, 1985.
932 Lee, X.: On micrometeorological observations of surface-air exchange over tall
933 vegetation, Agric. For. Meteorol., 91, 39-49, 1998.
934 Lennaert van, V., Shigeo, K., and Genta, K.: Periodic motion representing isotropic
935 turbulence, Fluid Dyn. Res., 38, 19–46, 2006.
936 Li, X., Hu, F., Pu, Y., Al-Jiboori, M. H., Hu, Z., and Hong, Z.: Identification of
937 coherent structures of turbulence at the atmospheric surface layer, Adv. Atoms.
938 Sci., 19(4), 687-698, 2002.
939 Mahrt, L., Ek, M.: Spatial variability of turbulent fluxes and roughness lengths in
940 HAPEX-MOBILHY, Bound. Lay. Meteor., 65, 381-400, 1993.
941 Malhi,Y., McNaughton, K., and Von Randow, C.: Low frequency atmospheric
942 transport and surface flux measurements, in: Handbook of micrometeorology,
943 Lee, X., Massman, W. J., and Law, B., Springer, 101-118, 2004.
944 Martano, P.: Estimation of surface roughness length and displacement height from
945 single-level sonic anemometer data, J. Appl. Meteorol., 39(5), 708–715, 2002.

946 Mattingly, J. C.: On recent progress for the stochastic Navier Stokes equations,
947 Journées équations aux dérivées partielles, Univ. Nantes, Nantes, Exp. No. XI,
948 1-52, 2003.
949 McMillen, R. T.: An eddy correlation technique with extended applicability to non
950 simple terrain, Bound. Lay. Meteor., 43, 231-245, 1988.
951 Moore, C. J.: Frequency response corrections for eddy correlation systems, Bound.
952 Lay. Meteor., 37, 17-35, 1986.
953 Neumann, J. V.: Proof of the quasi-ergodic hypothesis, Mathematics Proc. N. A. S.,
954 18, 70-82, 1932.
955 Padro, J.: An investigation of flux-variance methods and universal functions applied
956 to three land-use types in unstable conditions, Bound. Lay. Meteor., 66, 413–425,
957 1993.
958 Panofsky, H, A,, Lenschow, D, H,, and Wyngaard, J. C.: The characteristics of
959 turbulent velocity components in the surface layer under unstable conditions. Bound.
960 Lay. Meteor., 11, 355–361, 1977.
961 Papoulis A. and Pillai S. U.: Probability, random variables and stochastic processes.
962 McGraw-Hill. New York. 666, 1991.
963 Poulos, G. S., Blumen, W., Fritts, D, C., Lundquist, J. K., Sun, J., Burns, S. P., Nappo,
964 C., Banta, R., Newsom, R., Cuxart, J., Terradellas, E., and Balsley, Ben.: CASES-99:
965 a comprehensive investigation of the stable nocturnal boundary layer. Bull. Amer.
966 Meteor. Soc., 83, 555–581, 2002.
967 Running, S. W., Baldocchi, D. D., Turner, D. P., Gower, S. T., Bakwin, P. S., and
968 Hibbard, K. A.: A global terrestrial monitoring network integrating tower fluxes,
969 flask sampling, ecosystem modeling and EOS satellite data, Remote Sens. Environ.,
970 70(1), 108-127, 1999.

971 Sakai, R. K., Fitzjarrald, D. R., and Moore, K. E.: Importance of low-frequency
972 contributions to eddy fluxes observed over rough surfaces. J. Appl. Meteorol., 40,
973 2178–2192, 2001.
974 Schotanus, P., Nieuwstadt, F. T. M., and de Bruin, H. A. R.: Temperature measurement
975 with a sonic anemometer and its application to heat and moisture fluxes, Bound.
976 Lay. Meteor., 26, 81–93, 1983.
977 Segal, M., Avissar, R., McCumber, M. C., and Pielke, R. A.: Evaluation of vegetation
978 effects on the generation and modification of mesoscale circulations, J. Atmos.
979 Sci., 45, 2268-2292, 1988.
980 Staebler, R. M., Fitzjarrald, D. R.: Observing subcanopy CO_2 advection, Agric. Forest
981 Meteorol. 122, 139-156, 2004.
982 Stull, R. B.: An introduction to boundary layer meteorology. Kluwer Academic Publ.
983 Dordrecht. 670, 1988.
984 Sun, J., Desjardins, R., Mahrt, L., MacPherson, I.: Transport of carbon dioxide, water
985 vapor and ozone over Candle Lake, J. Geophys. Res., 103, 25873-25885, 1997.
986 Uffink, J.: Boltzmann'S wofk in statistical physics, Stanford encyclopedia of
987 philosophy, Edward, N. Z., 2004.
988 Webb, E. K., Pearman, G. I., and Leuning, R.: Correction of the flux measurements for
989 density effects due to heat and water vapour transfer, Q. J. R. Meteorol. Soc., 106,
990 85–100, 1980.
991 Wilczak, J. M., Oncley, S. P., Stage, S. A.: Sonic anemometer tilt correction
992 algorithms. Bound. Lay. Meteor., 99(1), 127-150, 2001.
993 Wyngaard, J. C.: Turbulence in the atmosphere, getting to know turbulence,
994 Cambridge University Press, 2010.
995 Zhang Q. and Li H.: The relationship between surface energy balance unclosure and

vertical sensible heat advection over the loess plateau, Acta Phys. Sin., 59(8), 5888-5895, 2010.

Zuo, H., Xiao X., Yang Q., Dong L., Chen J., Wang S.: On the atmospheric movement and the imbalance of observed and calculated energy in the surface layer, Sci. China. Ser. D-Earth Sci., 55(9), 1518-1532, 2012.

Table 1 Local Stability Parameter $(z\text{-}d)/L_c$ of the Eddies in Different Temporal Scales on August 25

Time / Eddy scale	3:00-4:00	7:00-8:00	14:00-15:00
≤2 min	0.59	0.52	-0.38
≤3 min	0.31	0.38	-0.44
≤5 min	0.28	0.16	-0.40
≤10 min	-0.01	0.15	-0.34
≤30 min	-0.04	-0.43	-0.27
≤60 min	-0.07	-1.29	-0.30

Table 2 Parameters of Similarity and Fitting Curve of Vertical Velocity Variance

	10 min		30 min		60 min	
	$z/L<0$	$z/L>0$	$z/L<0$	$z/L>0$	$z/L<0$	$z/L>0$
c_1	1.08	1.17	1.06	1.12	0.98	1.06
c_2	4.11	3.67	3.64	3.27	4.62	2.62
R	0.97	0.76	0.94	0.56	0.83	0.30
S	0.19	0.25	0.17	0.27	0.25	0.31

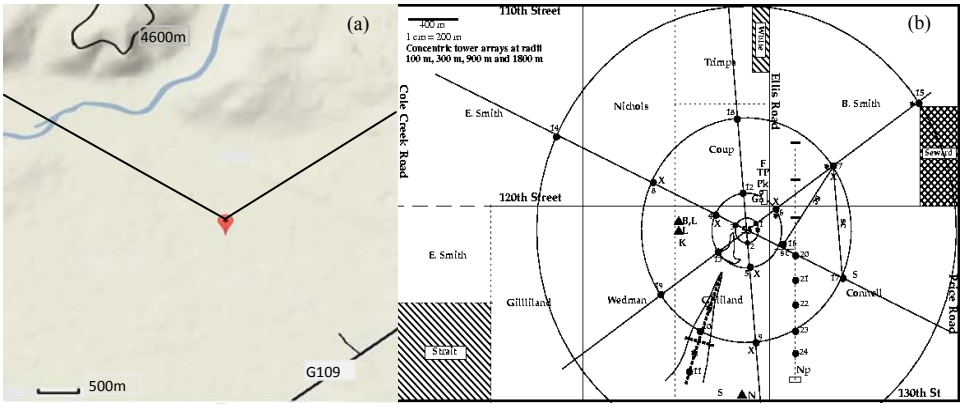

Figure 1. Overview diagram of Nagqu Station of Plateau Climate and Environment (a) and CASES-99 observation Station (b) (cited from Poulos, 2002).

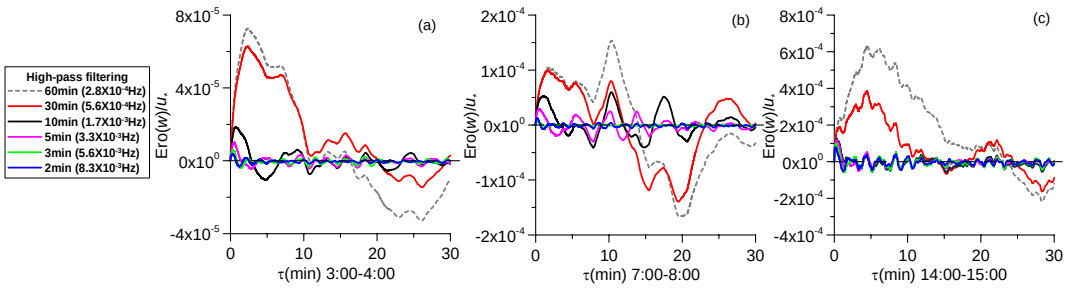

Figure 2. Variation of average ergodic function Ero(***w***) of eddies in different scales of vertical velocity measured at Nagqu Station at the height of 3.08 m in the three time frames with relaxation time. Panels (a), (b) and (c) are the respective results of the three time frames. If their average ergodic function is more approximate to zero, then the average of the eddies in the corresponding temporal scale will more closely satisfy the ergodic conditions.

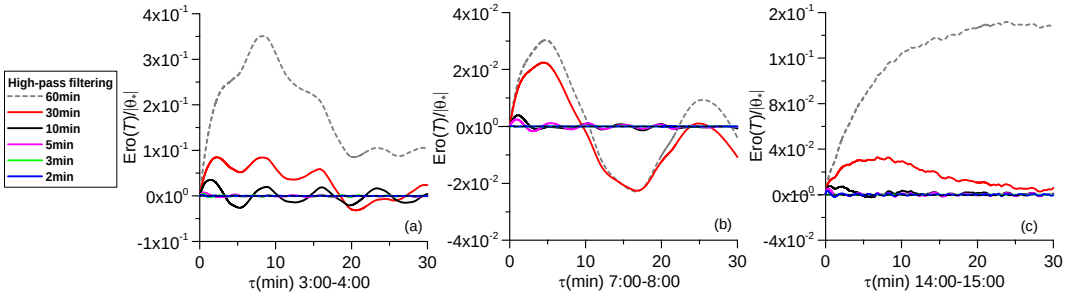

Figure 3. Variation of average ergodic function Ero(*T*) of the eddies in the different scales of temperature with relaxation time (other conditions are similar to Fig. 2, and the same applies to the following figures).

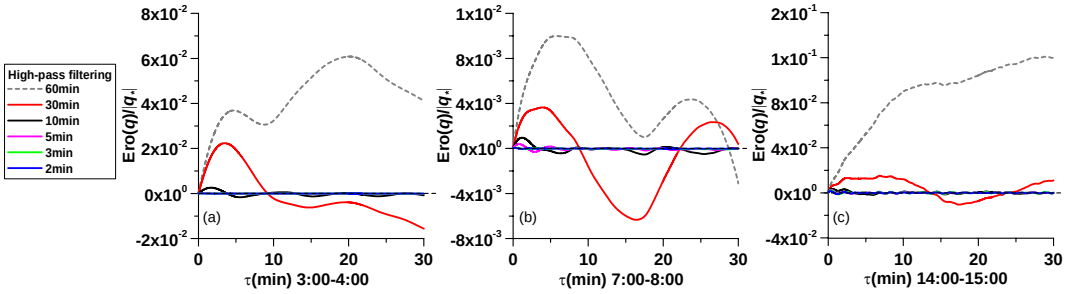

Figure 4. Variation of average ergodic function Ero(q) of the eddies in the different scales of humidity with relaxation time.

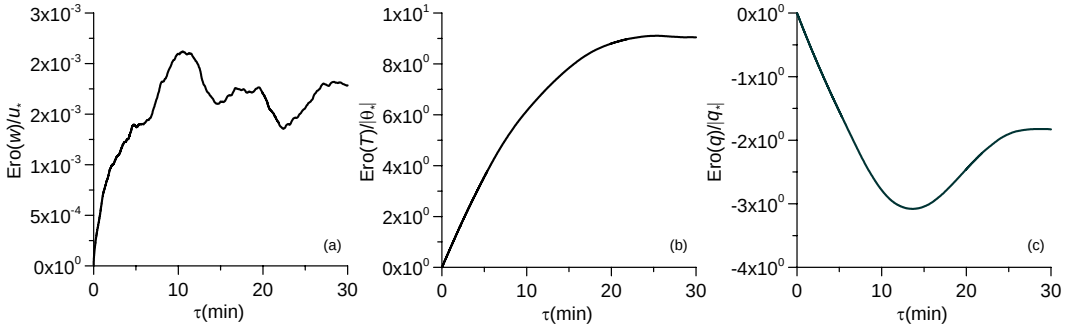

Figure 5. Variation of average ergodic function of unfiltered vertical velocity (a), temperature (b) and humidity (c) during 14:00-15:00 with relaxation time.

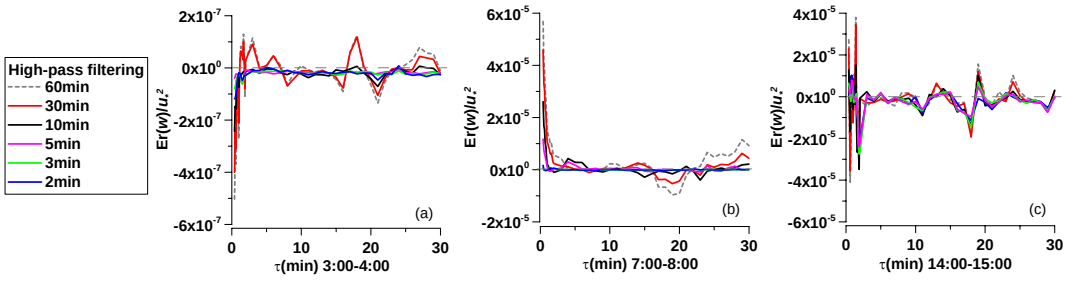

Figure 6. Variation of ergodic theorem of autocorrelation function of the eddies in the different scales of vertical velocity with relaxation time.

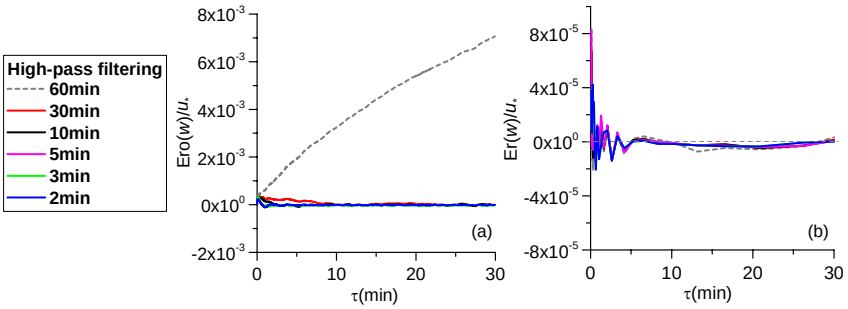

Figure 7. Variation of average ergodic function (a) and ergodic theorem of autocorrelation function (b) of the eddies in the different scales of the vertical velocity with relaxation time at the seven observation locations of CASES-99.

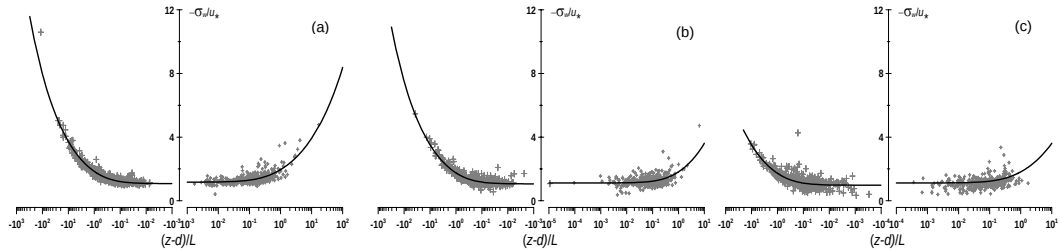

Figure 8. Similarity relation of vertical velocity variances of eddies in different scales of Nagqu; Panels (a), (b) and (c) respectively represent the similarity of eddies of 10 min, 30 min and 60 min in the temporal scale.

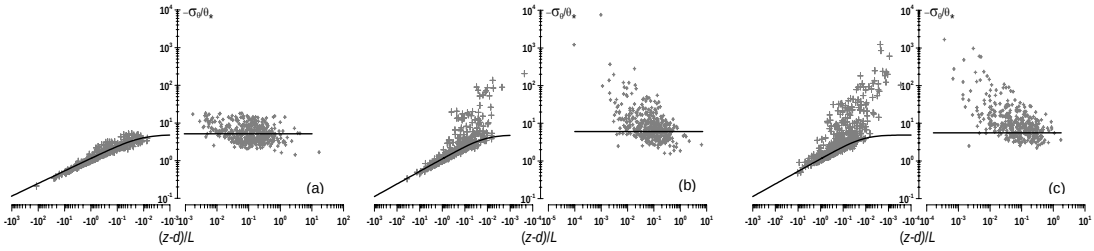

Figure 9. Similarity relations of temperature variance of eddies in different scales of Nagqu; Panels (a), (b) and (c) respectively represent the similarity of the eddies of 10 min, 30 min and 60 min in the temporal scale.